

Effect of Zn Addition on Clustering Behavior in a Pre-Aged Al-Mg-Si-Cu Alloy and Its Relation to Bake Hardening Response

Zhu Shang, Li Zhihui, Yan Lizhen, Li Xiwu, Huang Shuhui, Yan Hongwei,
Zhang Yongan, Xiong Baiqing

State Key Laboratory of Nonferrous Metals and Processes, GRINM Group Co., LTD., Beijing 100088, China

Abstract: The effect of Zn addition on clustering behavior in a pre-aged Al-Mg-Si-Cu alloy and its relation to bake hardening response were investigated. After pre-aging at 100 °C for 3 h, the Zn addition prompts the formation of clusters with a uniform Mg/Si ratio, which can easily transform into β'' phases. Consequently, a fine and dense distribution of β'' phases is observed in the Al-Mg-Si-Cu alloy with Zn addition during bake hardening treatment at 185 °C for 25 min after pre-aging. This correlates well with the enhanced bake hardening response of the Al-Mg-Si-Cu alloy with Zn addition.

Key words: Al-Mg-Si-Cu alloy; Zn addition; clustering behavior; bake hardening response

Al-Mg-Si alloys have been widely used as automotive body panels due to their desirable combination of excellent formability, good corrosion resistance and high strength-to-weight^[1,2]. These alloys display a significant increase in hardness during paint baking cycle, referred to as the bake hardening (BH) response, which is attributed to the formation of GP zones, pre- β'' or β'' phases that hind dislocation movement in the host material^[3-5]. Unfortunately, the relatively low temperature and short holding time of the typical paint baking processes (170~185 °C for 20~30 min) cannot fully exploit the age hardening potential of the Al-Mg-Si alloys. Besides, in practical manufacture, storing Al-Mg-Si alloys at room temperature prior to paint baking is usually unavoidable and thus natural aging (NA) would happen. This generates two problems for industrial application of Al-Mg-Si alloys. First, the formation of clusters during NA results in the enhanced strength, which can reduce formability during stamping^[6]. Second, these clusters cause the so-called negative effect of NA on BH response^[7,8]. The reason of this negative effect can be well understood as follows^[9-13]: (1) the clusters formed during NA not being favourable nucleation sites for β'' phases and

dissolving in paint baking condition, (2) lower solute concentrations in matrix inhibiting nucleation of suitable precursors of β'' phases, and (3) lower solute diffusivity due to a drop in vacancy concentration as NA clusters acting as vacancy sinks. The basic requirement for automotive body panels is to have a good formability during stamping process and preferably increasing in strength after paint-baking cycle. Hence, maximal suppression of NA and remarkable improvement in BH response are essential for successful application of Al-Mg-Si alloys in automotive industry.

Nowadays, additions of other alloying elements to Al-Mg-Si alloys and pre-aging treatment immediately after quenching have been developed to improve the mechanical properties of these alloys. The effects of Cu addition on precipitation microstructures and mechanical properties of Al-Mg-Si alloys have been extensively studied. The addition of Cu leads to the formation of L/S/C, QP and QC phases, which contribute to a significant hardening effect^[14,15]. The presence of Cu can also suppress the negative effect of NA. The incorporation of Cu atoms into NA clusters minimizes the strain energy caused by the difference in atomic sizes, changing the stability of these clusters^[16,17].

Received date: November 25, 2018

Foundation item: National Key R&D Program of China (2016YFB0300802)

Corresponding author: Li Zhihui, Ph. D., Professor, State Key Laboratory of Nonferrous Metals and Processes, GRINM Co., LTD, Beijing 100088, P. R. China, Tel: 0086-10-60662656, E-mail: lzh@grinm.com

Copyright © 2019, Northwest Institute for Nonferrous Metal Research. Published by Science Press. All rights reserved.

This facilitates their transformation into β'' phases^[17]. Therefore the effect of NA is less deleterious to subsequent BH response. However, the Cu-containing alloys usually exhibit inferior formability^[17]. Besides Cu addition, pre-aging (PA) treatment has also been used to enhance BH response and to suppress hardening during NA. It is known that clusters with a uniform Mg/Si are formed during PA and they can easily transform into β'' phases at paint baking temperature, leading to an enhanced BH response^[4, 9]. The formation of clusters during PA results in the lower vacancy and solute concentrations, which prevent formation of clusters during subsequent NA^[4,8]. As a consequence, PA has an mitigating influence on the negative effect of NA.

Some recent works confirm that the addition of Zn to Al-Mg-Si-Cu alloy is able to induce enhanced age hardening response, due to the increase in number density of β'' phase or multi-phase hardening effects by the coexistence of GP zones, β'' phase, GP (II)-zones of η -MgZn₂ and η' phase^[18-22]. However, there are very few reports about the clustering during pre-aging and its effect on subsequent BH behavior in Zn-containing Al-Mg-Si-Cu alloy. In this paper, the focus is made on the role of Zn addition to an Al-Mg-Si-Cu alloy in the clustering behavior during pre-aging and the influence of this on the subsequent BH response.

1 Experiment

Two kinds of Al-Mg-Si-Cu alloys with and without Zn addition, named as the Zn-added and Zn-free alloys, were used in this study. Their chemical compositions are listed in Table 1. The alloy ingots were homogenized at 430 °C for 10 h plus 545 °C for 16 h in an air furnace, then hot and cold rolled to sheets with the final thickness of 1.0 mm. The alloy sheets were solution treated at 550 °C for 0.5 h in a muffle furnace followed by quenching into water at room temperature. Then PA treatment was conducted at 100 °C for 3 h. The pre-aged samples were subsequently aged in an air-circulation oven at 185 °C for 25 min to check the BH response. The hardness was measured by a Vickers hardness tester at a load of 5 kg with a dwell time of 10 s. The data points were determined from the average of at least 10 indentations.

Thin foils for transmission electron microscopy (TEM) study were prepared by twin-jet electropolishing with an consisting of 30 vol% nitric acid in methanol solution. The

Table 1 Chemical composition of the experimental alloys (wt%)

Alloy	Mg	Si	Zn	Cu	Mn	Zr	Fe	Al
Zn-free	0.90	0.82	0.01	0.23	0.11	0.09	<0.1	Bal.
Zn-added	0.92	0.78	0.64	0.23	0.10	0.12	<0.1	Bal.

electrolyte temperature was kept blew -30 °C. A potential of 15 V produced a current of approximately 50 mA during the thinning. The TEM observation was performed using a TecnaiG2 F20 operated at 200 kV. Quantitative analysis was conducted on TEM bright-field images. The thickness of the thin foil was required for quantitative calculation and measured by contamination spot separation (CSS) method^[23]. Details about the microstructural measurements can be given elsewhere^[24].

Three-dimension atom probe (3DAP) study was carried out by a LEAPTM 4000 HR instrument with a detector efficiency of 36%. The square bars for 3DAP test were cut from the sheets and electropolished using a standard two stage method. The 3DAP experiments were performed at a specimen temperature of 20 K with a pulse fraction of 20% and a pulse rate of 200 kHz. IVAS 3.6.12 software was used to do three dimensional reconstruction and data analyses. The maximum separation algorithm was employed to identify clusters^[25], in which the minimum number of solute atoms (N_{min}) was set to 10, and the other three parameters, including the maximum distance between atoms (D_{max}), the surround distance (L) and the erosion distance (S), were set to 0.7 nm for a meaningful detection of nearest neighbour atoms. In addition, the radius of gyration and the associated Guinier radius^[26] were used to define the sizes of the clusters.

2 Results and Discussion

2.1 Hardness measurements

The hardness results of experimental alloys after different heat treatments are presented in Fig.1. The hardness (HV) after the PA treatment is about 780 MPa for Zn-free alloy and 790 MPa for Zn-added alloy. When the BH treatment is introduced, the hardness (HV) is about 1060 MPa in Zn-free alloy and 1150 MPa in Zn-added alloy. The increased hardness of Zn-added alloy during BH treatment is 80 MPa higher than that of Zn-free alloy, implying that an enhanced BH response is achieved by Zn addition.

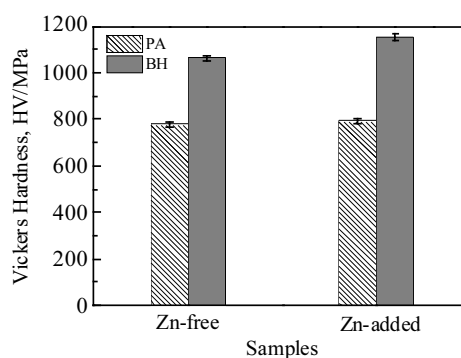


Fig.1 Vickers hardness of the Zn-free and Zn-added alloys during pre-aging (PA) at 100 °C for 3 h and subsequent bake hardening (BH) treatment at 185 °C for 25 min (stated errors represent one standard error on the basis of ten measurements per sample)

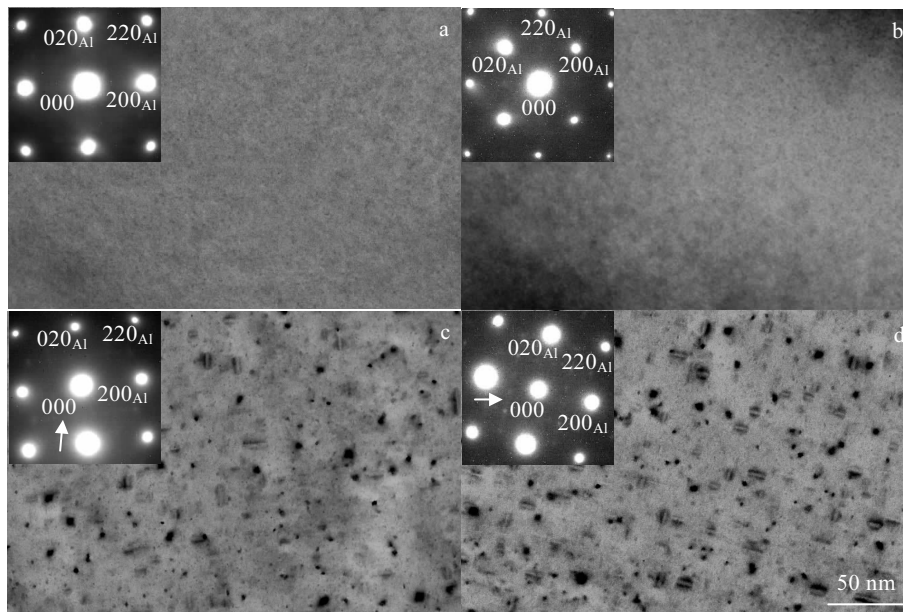


Fig.2 TEM bright field images and (001) SAED patterns obtained from experimental alloys in different heat treatment conditions: (a, b) pre-aging (PA) at 100 °C for 3 h; (c, d) bake hardening (BH) treatment at 185 °C for 25 min after PA; (a, c) Zn-free alloy; (b, d) Zn-added alloy (white arrow points to extra streaks in Fig.2c and 2d)

2.2 TEM observations

TEM bright field images and (001) SAED patterns for the Zn-free and Zn-added alloys in different heat treatment conditions are displayed in Fig.2. After PA at 100 °C for 3 h, there is no indication of precipitate in the bright field images of the Zn-free and Zn-added alloys as shown in Fig.2a and Fig.2b, respectively. This is consistent with only diffraction spots of the Al matrix observed in their SAED patterns. During BH treatment at 185 °C for 25 min after PA, a larger number of dot-like and needle-like precipitates are clearly visible in the Zn-free and Zn-added alloy as shown in Fig.2c and Fig.2d. The corresponding SAED patterns show extra streaks along the [001] directions, indicating that the needle-like precipitates can be identified as β'' phases. These dot-like precipitates are considered to be the β'' phase viewed end-on because their size is 3~4 nm, as suggested by Ding et al.^[5]. Note that the Zn-added alloy exhibits a finer and denser distribution of β'' phases compared with the Zn-free alloy. This result explains the enhanced BH response caused by Zn addition (Fig.1). The quantitative analysis of β'' phases in Zn-free and Zn-added alloys after BH treatment is summarized in Table 2. It is found that the Zn-added alloy has the higher number density and volume fraction of β'' phases with smaller size than Zn-free alloy.

The typical HRTEM image of an embedded β'' phase for Zn-added alloy in BH condition is shown in Fig.3a and Fig.3b is the corresponding FFT patterns. They clearly present that the β'' phase belongs to the monoclinic struc-

ture with lattice parameters $a=1.516$ nm, $c=0.674$ nm and $\beta=105.26^\circ$. The result is in good agreement with the report of Edward et al.^[1]. Further, the orientation relationship between the β'' phase and Al matrix is: $(010)\beta'' // (001)\text{Al}$, $[001]\beta'' // [310]\text{Al}$, and $[100]\beta'' // [\bar{2}30]\text{Al}$.

2.3 3DAP analysis

3DAP atom maps of Zn-free and Zn-added alloys after PA treatment are shown in Fig.4 and the average solute concentration of clusters in the two alloys is given in Table 3. From Fig.4a and Fig.4b, it is evident that many small clusters are observed in the Zn-free and Zn-added alloys. The atom maps of typical small clusters in an enlarged view are shown in Fig.4c and Fig.4d. It is clear that Mg, Si and Cu atoms partition into the clusters of the two alloys. In addition, Zn atoms also exhibit a preferential partitioning into the clusters of Zn-added alloy. The quantitative information in Table 3 confirms that the clusters of Zn-added alloy have an average Zn concentration of $(5.3 \pm 0.9)\text{at}\%$. Note that the average Cu concentration of clusters in the Zn-free and Zn-added alloys only fluctuates in the range from $(2.2 \pm 0.3)\text{at}\%$ to $(2.3 \pm 0.4)\text{at}\%$. This result means that the average Cu concentration

Table 2 Statistics of β'' phases in Zn-free and Zn-added alloys after bake hardening (BH) treatment

Alloy	Cross section/ nm^2	Length/ nm	Number density/ $\times 10^{22} \text{m}^{-3}$	Volume fraction/%
Zn-free	7.6 ± 0.8	9.2 ± 0.7	4.2 ± 0.7	0.24 ± 0.03
Zn-added	7.2 ± 0.5	6.8 ± 0.8	7.3 ± 0.4	0.35 ± 0.05

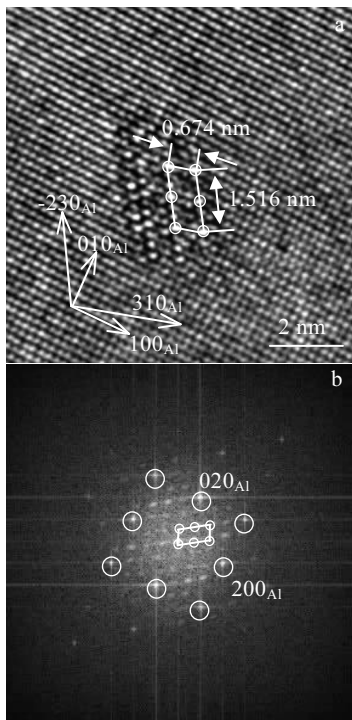


Fig.3 HRTEM image (a) and corresponding FFT pattern (b) of the β'' phase for Zn-added alloy in bake hardening (BH) condition

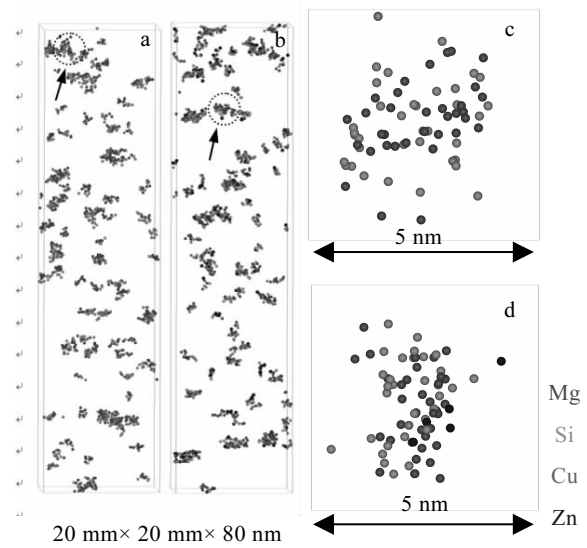


Fig.4 3DAP atom maps of experimental alloys after pre-aging (PA) at 100 °C for 3 h. Purple, green, yellow and blue dots represent Mg, Si, Cu and Zn atoms, respectively: (a) Zn-free alloy, (b) Zn-added alloy, (c) enlarged atom maps of individual cluster marked in circle in Fig.4a, and (d) enlarged atom maps of individual cluster marked in circle in Fig.4b

Table 3 Average solute concentration of clusters measured by 3DAP for Zn-free and Zn-added alloys after pre-aging (PA) at 100 °C for 3 h

Alloy	Average solute concentration in clusters/at%				Mg/Si ratio
	Mg	Si	Cu	Zn	
Zn-free	24.1 ± 5.1	32.2 ± 4.5	2.2 ± 0.3	-	0.75 ± 0.2
Zn-added	26.6 ± 3.5	26.1 ± 4.1	2.3 ± 0.4	5.3 ± 0.9	1.01 ± 0.1

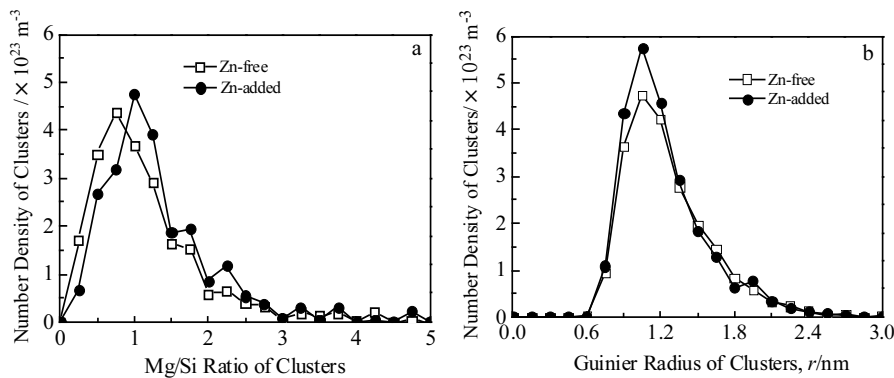


Fig.5 Number density of cluster vs Mg/Si ratio (a) and guinier radius (b) of clusters in the Zn-free and Zn-added alloys after pre-aging (PA) at 100 °C for 3 h

of clusters is independent on Zn addition. In contrast, the addition of Zn leads to an increase in the Mg/Si ratio of clusters.

After PA at 100 °C for 3 h, the size distribution of the clusters in the Zn-free and Zn-added alloys is shown in Fig.5a. A peak in number density can be seen at approxi-

mately 1.0 nm in Guinier radius for the two alloys. The radius of most of the clusters in the two alloys is not greater than 2.4 nm. Compared to the Zn-free alloy, a higher number density with radius ranging from approximately 0.9~1.2 nm can be observed in Zn-added alloy. The relationship of the Mg/Si ratio to the cluster number density of the Zn-free and

Zn-added alloys after PA treatment is shown in Fig.5b. For example, the Mg/Si ratio in the plot labeled 1.0 is in range from 0.75 to 1.0. The Mg/Si ratio of clusters in the two alloys is seen to vary between close to 0.0 and 5.0. The clusters with low Mg/Si ratio ($Mg/Si < 1.0$) are designed as Si-rich clusters and those with high Mg/Si ratio ($Mg/Si > 1.0$) are considered to be Mg-rich clusters. It is found that the number density of Si-rich clusters is higher in the Zn-free alloy than that in Zn-added alloy. However, clusters with Mg/Si ratio of 1.0 has the highest number density in the Zn-added alloy. The relationship between the Mg/Si ratio and size of clusters formed during PA treatment is shown in Fig.6. The clusters exhibit various Mg/Si ratio in the Zn-free and Zn-added alloys (Fig.6a and Fig.6b). This variation of Mg/Si ratio decreases with the increase of cluster size. The larger clusters have a narrow distribution of the Mg/Si ratio, approaching a ratio of 1.0 for Zn-added alloy and 0.75 for Zn-free alloy.

Based on the above analysis, it is reasonable to believe that Zn addition prompts the formation of clusters with a uniform Mg/Si ratio during PA treatment, with no significant change in the cluster size.

The clusters with a uniform Mg/Si ratio and Si-rich clusters play different roles in the formation of β'' phases. Due to the compositional similarity between the clusters with a uniform Mg/Si ratio and β'' phases, the clusters with a uniform Mg/Si ratio can transform easily into the β'' phases after paint baking cycle^[9]. On the contrary, the Si-rich clusters are believed to be difficult to evolve into the β'' phase and to dissolve at paint baking temperature because of the ion binding property for the

bonding of Si-Si atoms^[10]. After PA at 100 °C for 3 h, the addition of Zn stimulates the formation of clusters with a uniform Mg/Si ratio, which can directly transform into β'' phases during subsequent BH treatment. As a result, the refined distribution of β'' phases is observed in Zn-added alloy. However, compared with Zn-added alloy, the Zn-free alloy has a lower number density of clusters with a uniform Mg/Si ratio after PA treatment. This results in fewer nucleation sites for development of β'' phases. Moreover, the higher number density of Si-rich clusters leads to the lower solid solution concentration of atoms in the matrix because they are relatively stable at BH temperature. This lower solid solution concentration of atoms in matrix inhibits nucleation of suitable precursors of β'' phases. Therefore, for the Zn-free alloy experiencing BH treatment, β'' phases grow on reduced nucleation sites, leading to a coarse microstructure with lower number density and larger size. The Zn-free alloy thus has lower BH response.

The role of Zn in formation of the clusters with a uniform Mg/Si ratio during PA treatment is discussed as follows. It is known that the quenched-in vacancies are a key factor controlling the clustering kinetics during early stages of aging^[12, 27]. Because the binding energy between Si atoms and vacancies is more favorable than Mg atoms and Si atoms have a higher diffusion rate in Al matrix^[12]. Si-rich clusters form more easily in the early stages of aging, and Mg atoms can diffuse into the clusters until the uniform Mg/Si ratio is reached^[28]. On the other hand, it has been reported that the solute-vacancy binding energies of Mg, Si, Zn in Al alloys are -0.02, 0.08 and 0.03 eV, respectively^[19, 29]. These values are in good agreement with the experiment values: -0.01 eV for Mg, 0.03 eV for Si and 0.02 eV for Zn^[19, 30]. The capability of solute combining the vacancy can thus be described as: $Si > Zn > Mg$ ^[19]. Also, Zn has a strong interaction with Mg atoms. It has been calculated that Mg-Zn clusters have a formation enthalpy of -6.1 J/mol at 0 K, which are larger than that of Mg-Si clusters (-16.4 J/mol)^[31]. Therefore, for the Zn-added alloy, it should be deduced that Zn atoms can "steal" Mg atoms and quenched-in vacancies to form Mg-Zn cluster in the initial stage of PA. Then, the Mg-Zn clusters act as the effective nucleation sites for Si-rich clusters, leading to the denser distribution of Si-rich clusters. In other words, the average distance between Si-rich clusters becomes shorter. As a result, the migration time for Mg atoms to reach the pre-exist Si-rich clusters can be reduced. Therefore, the formation of the clusters with a uniform Mg/Si ratio is enhanced and accelerated by the Zn addition.

3 Conclusions

1) Zn addition enhances the BH response. Compared with Zn-free alloy, the Zn-added alloy has a higher increase in hardness during BH treatment at 185 °C for 25 min after PA at 100 °C for 3 h.

2) Zn addition stimulates the formation of β'' phases in BH condition. A finer and denser distribution of β'' phases

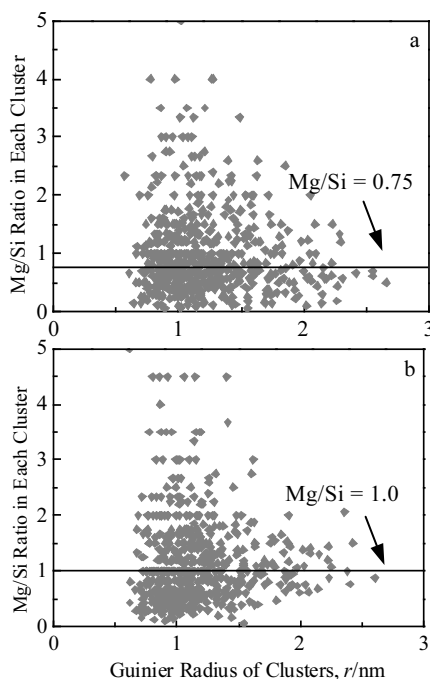


Fig.6 Relationship between Mg/Si ratio and Guinier radius of clusters for Zn-free alloy (a) and Zn-added alloy (b) after pre-aging (PA) at 100 °C for 3 h

can be observed in Zn-added alloy. This correlates well with the enhanced BH response caused by Zn addition. Based on the quantitative TEM analysis, Zn addition increases the volume fraction and number density of β'' phases while decreases their cross section and length.

3) Zn addition prompts the formation of clusters with a uniform Mg/Si ratio after PA treatment. It is believed that the addition of Zn enhances the formation of Si-rich clusters and then reduces the migration time for Mg atoms to reach the pre-exist Si-rich clusters. Thus the more clusters with a uniform Mg/Si ratio can be formed rapidly during PA. The clusters with a uniform Mg/Si ratio can easily transform into β'' phases at BH temperature. Accordingly, Zn addition stimulates the formation of β'' phases in the Al-Mg-Si-Cu alloy during BH treatment after PA.

References

- Edwards G A, Stiller K, Dunlop G L et al. *Acta Materialia*[J], 1998, 46: 3893
- Pogatscher S, Antrekowitsch H, Leitner H et al. *Acta Materialia*[J], 2011, 59: 3352
- Murayama M, Hono K, Miao W F et al. *Metallurgical and Materials Transactions A*[J], 2001, 32: 239
- Aruga Y, Kozuka M, Takaki Y et al. *Metallurgical and Materials Transactions A*[J], 2014, 45: 5906
- Ding L P, He Y, Wen Z et al. *Journal of Alloys and Compounds*[J], 2015, 647: 238
- Prillhofer R, Rank G, Berneder J et al. *Materials*[J], 2014, 7(7): 5047
- Zhen L, Kang S B. *Scripta Materialia*[J], 1997, 36: 1089
- Torsæter M, Hasting H S, Lefebvre W et al. *Journal of Applied Physics*[J], 2010, 108: 073527
- Serizawa A, Hirose S, Sato T. *Metallurgical and Materials Transactions A*[J], 2008, 39: 243
- Aruga Y, Kozuka M, Takaki Y et al. *Materials Science and Engineering A*[J], 2015, 631: 86
- Cuniberti A, Tolley A, Castro R M V et al. *Materials Science and Engineering A*[J], 2010, 527: 5307
- Banhart J, Chang C S T, Liang Z Q et al. *Advanced Engineering Materials*[J], 2010, 12: 559
- Zandbergen M W, Xu Q, Cerezo A et al. *Acta Materialia*[J], 2015, 101: 136
- Marioara C D, Andersen S J, Stene T N et al. *Philosophical Magazine*[J], 2007, 87: 3385
- Ding L, Jia Z, Liu Y et al. *Journal of Alloys and Compounds*[J], 2016, 688: 362
- Zandbergen M W, Cerezo A, Smith G D W. *Acta Materialia*[J], 2015, 101: 149
- Weng Y Y, Jia Z H, Ding L P et al. *Journal of Alloys and Compounds*[J], 2017, 695: 2444
- Cai Y H, Wang C, Zhang J S et al. *International Journal of Minerals, Metallurgy and Materials*[J], 2013, 20: 659
- Guo M X, Zhang Y, Zhang K W et al. *Materials Science and Engineering A*[J], 2016, 669: 20
- Yan L Z, Zhang Y A, Li X W et al. *Progress in Natural Science: Materials International*[J], 2014, 24: 97
- Ding X P, Cui H, Zhang J X et al. *Materials and Design*[J], 2015, 65: 1229
- Saito T, Wenner S, Osmundsen E et al. *Philosophical Magazine*[J], 2014, 94: 2410
- Andersen S J. *Metallurgical and Materials Transactions A*[J], 1995, 26: 1931
- Marioara C D, Andersen S J, Zandbergen H W et al. *Metallurgical and Materials Transactions A*[J], 2005, 36: 691
- Vaumousse D, Cerezo A, Warren P J. *Ultramicroscopy*[J], 2003, 95: 215
- Miller M K. *Atom Probe Tomography*[M]. New York: Kluwer Academic/Plenum Publishers, 2000
- Liu M, Čížek J, Chang C S T et al. *Acta Materialia*[J], 2015, 91: 355
- Fallah V, Langelier B, Ofori O P et al. *Acta Materialia*[J], 2016, 103: 290
- Wolverton C. *Acta Materialia*[J], 2007, 55: 5867
- Balluffi R W, Ho P S. *Diffusion Metals Park*[M]. OH: Am Soc Metals, 1973: 83
- Wolverton C. *Acta Materialia*[J], 2001, 49: 3129

Zn 添加对预时效态 Al-Mg-Si-Cu 合金原子团簇行为和烤漆硬化响应的影响

朱 上, 李志辉, 闫丽珍, 李锡武, 黄树晖, 闫宏伟, 张永安, 熊柏青
(有研科技集团有限公司 有色金属材料制备加工国家重点实验室, 北京 100088)

摘要: 通过显微硬度、透射电镜和三维原子探针表征测试手段, 研究了 Zn 添加对预时效态 Al-Mg-Si-Cu 合金原子团簇行为和烤漆硬化响应的影响。结果表明, 经 100 °C/3 h 预时效处理后, 含 Zn 和不含 Zn 合金中均形成了 Mg-Si 原子团簇。然而, 与不含 Zn 的合金相比, 含 Zn 合金中 Mg-Si 原子团簇数量更多, 表明 Zn 添加促进了 Mg-Si 原子团簇的形成。经 185 °C/25 min 烤漆处理后, 2 个合金在预时效过程中形成的 Mg-Si 原子团簇转变为具有明显增强效果的 β'' 相, 对应的烤漆增量也明显增加。由于预时效后的含 Zn 合金中 Mg-Si 原子团簇数量更多, 这为烤漆过程中 β'' 的形成提供了更多的形核核心。因此, 含 Zn 合金 β'' 相的尺寸更小, 分布更致密, 相对应的烤漆硬化响应速率也得以增强。

关键词: Al-Mg-Si-Cu 合金; Zn 添加; 原子团簇; 烤漆硬化

作者简介: 朱 上, 男, 1989 年生, 博士, 有研科技集团有限公司有色金属材料制备加工国家重点实验室, 北京 100088, 电话: 010-60662656, E-mail: zhushang_2015@163.com